

Optimal design of electrical power distribution grid spacers using finite element method

Stéfano Frizzo Stefenon^{1,2}  | Laio Oriel Seman³  | Bruno Antonio Pavan⁴  |
Raúl García Ovejero⁵  | Valderi Reis Quietinho Leithardt^{6,7} 

¹ Fondazione Bruno Kessler, Povo, Trento, Italy

² Computer Science and Artificial Intelligence, University of Udine, Udine, Italy

³ Graduate Program in Applied Computer Science, University of Vale do Itajaí, Itajaí, Brazil

⁴ Electrical Engineering Department, University of Planalto Catarinense, Lages, Brazil

⁵ Expert Systems and Applications Lab., E.T.S.I.I. of Béjar, Universidad de Salamanca, Salamanca, Spain

⁶ COPELABS, Lusófona University of Humanities and Technologies, Lisboa, Portugal

⁷ VALORIZA, Research Center for Endogenous Resources Valorization, Instituto Politécnico de Portalegre, Portalegre, Portugal

Correspondence

Stéfano Frizzo Stefenon, Fondazione Bruno Kessler, Via Sommarive 18, 38123 Povo, Trento, Italy.
Email: sfrizzostefenon@fbk.eu

Funding information

Fundación M. D. Samuel Solórzano Barruso, Grant/Award Number: FS/27-2020; FCT-PT/VALORIZA, Grant/Award Number: UIDB/05064/2020; FCT-PT/COFAC/ILIND/COPELABS/3/2020, Grant/Award Number: UIDB/04111/2020

Abstract

Spacers in the compact power distribution network are essential components for the support, organization, and spacing of conductors. To improve the reliability of these components and have an optimized network design, it is necessary to evaluate the performance of the variation of their geometric parameters. The analysis of these components is fundamental, considering that there are several models available that are validated by the electric power utilities. Due to the various possible design shapes, it is necessary to use an optimized model to reduce the electric potential located in specific sites, improving the reliability in the component, as the higher electrical potential results in a greater chance of failure to occur. The finite element method (FEM) stands out for evaluating the distribution of electrical potential. In this paper, an FEM is used to evaluate variations in vertical and horizontal dimensions in spacers used in the 13.8 kV power grid. The models are analyzed in relation to their behavior regarding the potential distribution on their surface. From the results of these variations, the model is optimized by means of a mixed-integer linear problem (MILP), replacing the FEM output with a ReLU network substitute model, to obtain a spacer with more efficiency to be used in semi-insulated distribution networks.

1 | INTRODUCTION

The electricity sector is constantly adapting to improve the quality of the electricity supply [1]. Some changes have an impact on its use, such as the growth of cities, increase in electricity consumption, and risk of accidents in places close to distribution networks [2]. Seeking ways to distribute electrical energy with less visual impact and better electrical insulation, the compact distribution network was developed. The compact network adds efficiency and a competitive cost compared to conventional networks [3].

Because the distribution networks are mostly overhead and are close to trees and buildings, bare conductors represent a risk

around the installations, given the possibility of discharges to the ground [4]. The trend is for new construction works on electrical extensions outside cities, subdivisions, and condominiums to have a compact network, instead of the conventional network. To improve the analysis of the components of the compact network, the finite element method (FEM) can be applied, being promising for the analysis of variations in the network components [5].

FEM consists of computational analysis, in which a solid is divided into several small parts. So the elements are added together to create a representation of the entire object being evaluated [6]. Through this approach, the application of electrical voltage is simulated at specific locations on the part being

This is an open access article under the terms of the [Creative Commons Attribution-NonCommercial License](https://creativecommons.org/licenses/by-nc/4.0/), which permits use, distribution and reproduction in any medium, provided the original work is properly cited and is not used for commercial purposes.

© 2022 The Authors. *IET Generation, Transmission & Distribution* published by John Wiley & Sons Ltd on behalf of The Institution of Engineering and Technology

analyzed, generating a potential difference. Based on this variation, it is possible to evaluate the behavior of the solid in terms of potential distribution over its surface and thus determine critical points and improve the component's design [7].

According to Orosz et al. [8], there are several techniques that could be applied to optimize the design of electric equipment based on FEM. The task to be faced in this research is that the global minimum is not guaranteed in the non-linear optimization problems making this a challenge. Some methods that could successfully be applied to design optimization of electrical equipment are: particle swarm optimization (PSO) [9] genetic algorithm (GA) [10], proxy models (PM) [11], covariance matrix adaptation evolution strategy (CMA-ES) [12], firefly algorithm (FA) [13], cuckoo search (CS) [14], among other optimization methods.

Through FEM, it is possible to evaluate elements with non-linear surfaces through the analysis of small parts of the object, thus evaluating the entire element in relation to a mesh of several nodes [15]. Other numerical methods have been studied to solve complex mathematical problems, currently, optimization methods have gained space in this context [16].

The use of advanced analysis methods has been applied to improve the reliability of electric energy distribution systems [17–19]. FEM can be applied for evaluating high voltage transmission lines with high electric field strength [20], which is promising due to the difficulty indirect measurements in the system and the high cost of producing prototypes in view of its insulation required for high voltage levels [21].

According to Yang et al. [22], parallel computing techniques are an alternative to improve FEM processing power. Genuine methods such as the black-box transmission line method improve the efficiency in analyzing the mesh. The transmission line method applied to finite element analysis can improve 50 times speedup within this evaluation an error of less than 2% [23].

A common problem in outdoor electrical power systems is the accumulation of contaminants on the surface of the insulators, the contamination reduces the insulating capacity of the network components, which results in electrical discharges [24]. FEM is successfully applied for analysis of room temperature vulcanizing for evaluation of damaged insulator pollution layer where leakage currents develop [25]. According to Guo et al. [26], the use of FEM is even applied to the analysis of complex systems such as the gas-insulated transmission lines.

Many authors have studied the influence of the accumulation of contaminants on the components of the electrical power system [27–29]. The contamination may result in an increase of the leaked current and the development of a fault [30]. Computational techniques are increasingly helping to identify adverse conditions to mitigate failures in the electrical power system [31]. According to Ghiasi et al. [32], the use of FEM to assess the level of contamination is promising, due to the possibility of variation in the profile, materials in simulation [33].

FEM is an approach that allows you to optimize the development of projects for the electrical power system, which can be applied to complex equipment such as power transformers [34], being possible to simulate thermal stress [35], galloping

features of transmission lines [36], and variations of the electric field [37]. In addition to the application for analysis of system components, FEM is used to assess equipment that may not be connected to the network and are important to keep the network working [38].

According to Ayodele, Ogunjuyigbe, and Oyewole [39] the FEM is a promising approach to apply in earthing grid system. Variations of the shape of the grid configuration based on the FEM can determine the best configuration with lower resistance. In addition to the analysis of the shape, the FEM can be applied to evaluate the frequency-dependent characteristic to determine the grounding performance in substations [40].

FEM has been applied to structure optimization for various applications [41]. These applications are directly related to improvement in equipment design [42–44], considering that through the finite element method it is possible to carry out evaluations of force distribution, temperature, and stress in complex structures [45]. Applications of this approach extend to high voltage power systems [46], using FEM makes it possible to assess process deterioration in electrical systems [47].

Based on the advantages of applying FEM for the analysis of electrical power system components, this paper will focus on the analysis of compact network spacers, which are components responsible for the support and spacing of conductors. Currently, there are several types of compact network spacers. Each manufacturer defines its model according to the requirements of the energy concessionaires responsible for the networks to be installed. However, it is not a definition of all dimensions of the component in a standardized way, which causes a difference in dimensions between manufacturers. For this reason, evaluating optimized dimensions which result in a lower electric potential at specific points can improve the design of spacers for compact networks.

The contribution of this paper is related to the improvement in the design of distribution spacers in the project phase. This improvement is given by the optimization of the dimension parameters based on the result of the application of FEM. The FEM is used to compute the electric potentials based on the variation of the design shape. To reduce the computational effort the element mesh is generated by an adaptive method which defines the size of the elements given the required computational cost needed to calculate it. Using an optimized model is obtained the constructive aspects for the design, reducing the electric potential on the component to mitigate failures.

The novelty of this paper is related to the evaluation of compact distribution networks. This type of distribution grid is being increasingly used because it has semi-isolated conductors. It is a safer system than conventional networks, very promising to be installed in areas with many trees. Thus, in this work, by using a neural network model to optimize the spacer parameters through the FEM results, it provides an opportunity for research on this type of network using a well-structured model that can be applied to the evaluation of other components.

The continuation of this paper is presented as follows: In Section 2 an explanation of the spacer function in compact distribution networks is presented. In Section 3 the method used in this

paper is presented. In Section 4 the results of using the method are discussed and finally, in Section 5 a conclusion is presented.

2 | COMPACT ELECTRIC DISTRIBUTION NETWORK

The compact electricity distribution network has been widely used in Brazil due to its advantages in terms of potential isolation [3], as the network is semi-isolated, which results in greater security for both people and the distribution system itself. Another advantage of the compact network is the low visual impact as it takes up less space in the distribution system [48].

The compact network is made up of aluminum or copper cables covered with a polymeric material, which prevents other bodies from touching directly on the conductive material [49]. If compared to the conventional distribution network, its cost is higher, as in the conventional network the conductors are naked [50]. Despite the higher cost, the compact network results in more system reliability. Another advantage of the compact network in relation to the conventional one is with regard to its installation and maintenance since the components are made of polymeric material, being lighter [51].

Ideal use for compact networking is in wooded areas, or places that are subject to elements that can come in contact with electrical power cables and cause shutdowns. According to Arantes Monteiro et al. [52] one of the biggest problems in the electricity distribution networks is the discharges to the ground, which occur when trees touch the network and there is a discharge to the ground. This problem can be avoided by using a semi-insulated network [53].

As with other types of distribution networks, the compact network is also subject to electromagnetic interference, atmospheric discharges, and induced voltages, which can cause high levels of voltage surges to break its insulation, causing failures [54]. For the problem to be minimized, it is necessary to ground the messenger conductor that runs along the entire length of the network together with the phase conductors, in a structure as shown in Figure 1.

Initially, the presented spacer has a vertical dimension of 400 mm and a horizontal dimension of 255 mm, being these the minimum dimensions for this component defined by the electric power utility [55]. Among the components that make up the structure of the compact network, the lozenge spacer, presented in Figure 1, is responsible for supporting and separating the cables in the network along the span (distance between two poles) keeping the distance of the electrical potential. This component is constructed of polymeric high-density polyethylene material and is the focus of the research of this paper.

2.1 | Component analysis

For the analysis of the electric field in the spacers of the compact network through the FEM, it is first necessary to elaborate the three-dimensional design of the spacer, with the appropri-

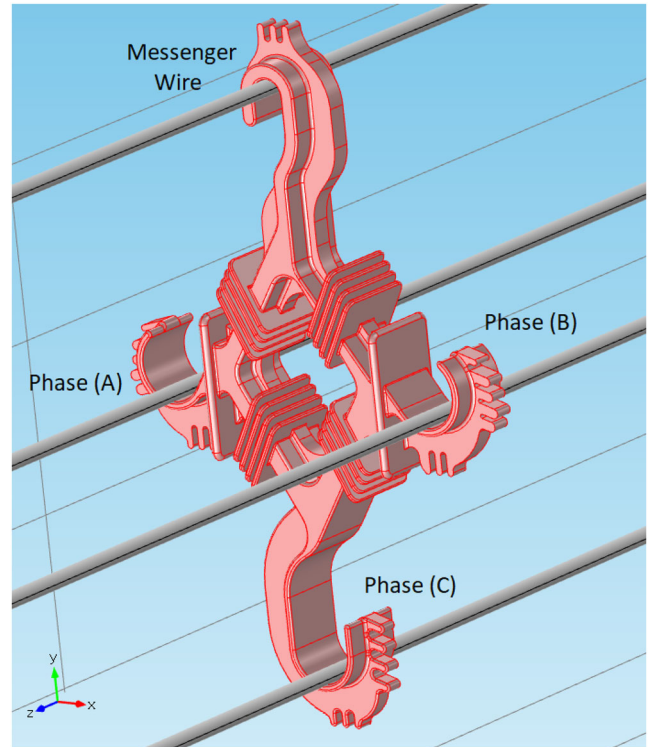


FIGURE 1 Cable identification in a compact network structure

ate medium voltage cables. For a proper evaluation of the component, its characteristics are observed in accordance with the approval of the local electricity concessionaire *Centrais Elétricas de Santa Catarina* (CELESC), specifically, the manual E-313.0045 [55].

After the model is designed in *SolidWorks* software, the files are imported and the parameterization of the finite element software started. In the 3D drawings stage, the dimensions of the spacer are defined based on the variations to be evaluated. In this paper, the cables used are aluminum with a relative permittivity equal to 8.5. The material considered for the spacer is high-density polyethylene with a relative permittivity of 2.26 [56], this material was also considered for all insulating parts. After defining the characteristics of the material, the potential is applied to the conductors. The electrical voltage values considered in this work are root mean square (RMS) values. As the phase-to-phase line voltage applied to the network is 13.8 kV (RMS), the phase-to-ground voltage is 7.97 kV (RMS). Thus, this voltage was applied to each of the spacer phase cables, and zero volts in the messenger cable, which is considered as a reference for grounding.

The material used for the spacer in compact networks and considered in this paper is high-density polyethylene. This composite is highly resistant to electric tracking and ultraviolet radiation. Its advantages are its high mechanical strength and flexibility against dynamic loads, being resistant to knocks and impacts. The extra-fine mode results in an analysis with greater precision that requires more computational effort [57]. After establishing the parameters, simulations and analysis began, which will be discussed in the following sections.

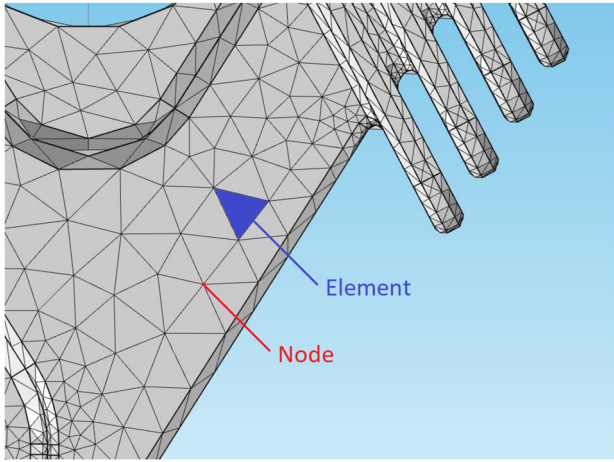


FIGURE 2 Node and element in simulated object using FEM

3 | FINITE ELEMENT METHOD

The finite element method has been used for many years for many electrical power system applications [58–60]. Currently using computers with high processing capacity, it is possible to analyze highly non-linear surfaces, which makes its application promising for evaluating electrical power system components [61]. To perform the calculation of non-linear geometric shapes, the object is discretized forming several nodes that connect to form several elements without losing their original properties. To apply the method, the elements can have square, triangular, hexagonal shapes, depending on the characteristics of the object to be analyzed [62].

The accuracy of the analysis through the method depends on the number of divisions elements of the object. In Figure 2, an image of a spacer is presented, in which the discretization of the surface into triangular elements is performed. As can be seen, there is a difference in size between the elements, because the adaptive mesh defines the size of the elements according to the complexity of solving the computation at the specific sites.

To reduce computational effort, the geometry is reduced by dividing the surface area into smaller parts called elements, then variables that are difficult to analyze are replaced by elements that are well defined and easy to solve [63]. The elements are connected by the nodal points and form a mesh. Then, differential equations are applied in the variational form to assess the physical behavior on their surface [64].

The meshing strategy is based on the division of extra-fine elements using triangular elements. The discretization of elements to form the element mesh is given by Equations (1)–(10). The predefined element discretization (extra-fine) makes the element mesh adaptive to the design variation, thus, smaller elements are used in sites with higher complexity. The limit values for the extra-fine mode are presented in Table 1.

The accuracy of the method depends on the size of the elements and the number of nodes, however, the more accurate the simulation, the greater the data processing needed [65]. In this paper, the object discretization for the element mesh is given by:

TABLE 1 Element mesh limit values for the extra-fine mode

| Parameter | Value |
|------------------------------|--------|
| Maximum element size | 0.1050 |
| Minimum element size | 0.0045 |
| Maximum element growth rate | 1.35 |
| Resolution of curvature | 0.30 |
| Resolution of narrow regions | 0.85 |

$$W(p, \varpi) = \sum_j W_j N_j(p, \varpi) \quad 1 \leq j \leq S, \quad (1)$$

where S represents the number of nodes in the mesh, W_j is the coefficient of the test function applied at the node j , and N_j is the base function at the node. Thus, the object's domain is divided into a number of N finite elements [66].

The V_e potential distribution of the element is related to the set of elements so that the potential is continuous across the boundaries between the interrelated elements. The approximate solution for the entire region is given by:

$$V(x, y) \approx \sum_{e=1}^N V_e(x, y). \quad (2)$$

Using a polynomial approximation for triangular elements, we have:

$$V_e(x, y) = a + bx + cy. \quad (3)$$

For triangular elements, the potential V_{e1} , V_{e2} and V_{e3} at nodes 1, 2, and 3, respectively, is obtained by:

$$\begin{bmatrix} V_{e1} \\ V_{e2} \\ V_{e3} \end{bmatrix} = \begin{bmatrix} 1 & x_1 & y_1 \\ 1 & x_2 & y_2 \\ 1 & x_3 & y_3 \end{bmatrix} \begin{bmatrix} a \\ b \\ c \end{bmatrix}, \quad (4)$$

where the coefficients a , b , and c are determined by:

$$\begin{bmatrix} a \\ b \\ c \end{bmatrix} = \begin{bmatrix} 1 & x_1 & y_1 \\ 1 & x_2 & y_2 \\ 1 & x_3 & y_3 \end{bmatrix}^{-1} \begin{bmatrix} V_{e1} \\ V_{e2} \\ V_{e3} \end{bmatrix}. \quad (5)$$

Replacing Equation (5) in Equation (4), we obtain

$$V_e = [1 \ x \ y] \frac{1}{2A} [MET] \begin{bmatrix} V_{e1} \\ V_{e2} \\ V_{e3} \end{bmatrix}, \quad (6)$$

where MET is given by:

$$\begin{bmatrix} (x_2y_3 - x_3y_2) & (x_3y_1 - x_1y_3) & (x_1y_2 - x_2y_1) \\ (y_2 - y_3) & (y_3 - y_1) & (y_1 - y_2) \\ (x_3 - x_2) & (x_1 - x_3) & (x_2 - x_1) \end{bmatrix}. \quad (7)$$

Reorganizing the equations gives,

$$V_e = \sum_{i=1}^3 \alpha_i(x_i, y_i) V_{ei} \quad (8)$$

where,

$$\begin{aligned} \alpha_1 &= \frac{1}{2A} [(x_2y_3 - x_3y_2) + (y_2 - y_3)x + (x_3 - x_2)y], \\ \alpha_2 &= \frac{1}{2A} [(x_3y_1 - x_1y_3) + (y_3 - y_1)x + (x_1 - x_3)y], \\ \alpha_3 &= \frac{1}{2A} [(x_1y_2 - x_2y_1) + (y_1 - y_2)x + (x_2 - x_1)y]. \end{aligned} \quad (9)$$

Therefore, the area A of the element is given by:

$$2A = \begin{vmatrix} 1 & x_1 & y_1 \\ 1 & x_2 & y_2 \\ 1 & x_3 & y_3 \end{vmatrix}, \quad (10)$$

$$2A = (x_1y_2 - x_2y_1) + (x_3y_1 - x_1y_3) + (x_2y_3 - x_3y_2),$$

$$A = \frac{1}{2} [(x_2 - x_1)(y_3 - y_1) + (x_3 - x_1)(y_2 - y_1)].$$

The value of A is positive if nodes are numbered clockwise. From the use of smaller elements, it is possible to analyze a complex problem by dividing it into simpler problems, where each element is described by a differential equation to evaluate the behavior of the solid [67].

In this paper, the focus of the analysis is on the distribution of electrical potential along the surface. This analysis aims to determine the places where there is a greater electric field, and thus, greater vulnerability to disruptive discharges.

The electric field (E) can be defined by the negative of the electric potential (V) gradient, calculated by:

$$E = -\nabla V. \quad (11)$$

Using Maxwell's equation the electric field is given by:

$$\nabla E = \rho/\epsilon, \quad (12)$$

where ρ is the total electric charge density and ϵ is the electric permittivity.

Substituting the electrical field from Equation (11) into Equation (12), the Poisson equation is given by:

$$-\nabla \cdot (\epsilon \nabla V) = \rho \Rightarrow \nabla^2 V = -\rho/\epsilon, \quad (13)$$

when ρ is zero [68], the distribution of potential in (r, z) is:

$$\frac{\partial^2 v}{\partial r^2} + \frac{1}{r} \frac{\partial v}{\partial r} + \frac{\partial^2 v}{\partial z^2} = 0. \quad (14)$$

As defined by Anbarasan and Usa [69], considering a function $F(v)$ of the surface distribution:

$$F(v) = \frac{1}{2} \iint \left[\epsilon_r \left(\frac{dv}{dr} \right)^2 + \epsilon_z \left(\frac{dv}{dz} \right)^2 \right] dr dz, \quad (15)$$

$$F(v) = \frac{1}{2} \iint \epsilon |\nabla^* v|^2 ds, \quad (16)$$

the contribution of F in relation to V , considering the variance of the potential of node i in element e , is given by:

$$x_e = \frac{1}{2} \iint \left[\frac{\epsilon}{dv} \left(\left(\frac{dv}{dr} \right)^2 + \left(\frac{dv}{dz} \right)^2 \right) \right] dr dz, \quad (17)$$

$$x_e = \frac{\epsilon}{2} \iint \left[2 \frac{dv}{dr} \cdot \frac{d}{dv_i} \left(\frac{dv}{dr} \right) + 2 \frac{dv}{dz} \cdot \frac{d}{dz_i} \left(\frac{dv}{dz} \right) \right] dr dz. \quad (18)$$

The Equation (18) is evaluated in Equation (3), then the electrical potential of any arbitrary point within each subdomain is obtained. In this paper, the *COMSOL Multiphysics* software was used to perform the FEM analysis (including meshing) [70]. The electrical potential values resulting from the finite element analysis are the inputs to the optimization model, which aims to determine the best dimensions for the spacer that minimize the potential applied at the points defined in this project.

3.1 | Optimization method

The optimization problem to be computed in this paper is focused on reducing the electric potential at specific sites according to the variation of dimensions in the shape design of the spacer. The optimization process is performed based on the possible dimensional constraints for the component. The considered values of electric potential are obtained from the FEM previously described.

To optimize the data obtained from the FEM analysis, in this article we propose to use an exact optimization model in order to find the best potential to be used. In this context, we can use a surrogate model that best approximates the behavior of the original model while being less costly to optimize. Substitute models are built using data from simulations, tests, and experiments. They work like a black box [71], where what matters is not the simulation logic, but the relationship

between input and output. In this way, it is possible to represent complex functions or with an unknown mathematical formulation [72].

One of the most common substitute models to be used in an optimization scenario is the piecewise linearization (PWL) [73]. However, the computational complexity of the model increases with the number of inputs and/or outputs to be considered, along with the number of considered data points [74]. Another possibility for the creation of a substitute model is the use of a neural network, more specifically one with a ReLU (Rectified Linear Unit) activation function [75]. In this paper, we leverage the formulation presented by [76] to rewrite a ReLU neural network as a mixed-integer linear problem (MILP) by means of binary variables. When using the ReLU network as a surrogate model instead of a PWL, the number of binary variables is equal to the number of neurons being used in the network. That way, it is possible to keep the network within an adequate size that satisfies a trade-off between the computational effort for the optimization problem and the desired quality in the approximation.

Consider the general formulation of a MILP, given by:

$$\min c^T \mathbf{x} + b^T \mathbf{y} \quad (19a)$$

$$\text{s.t. } A_k \mathbf{x} + G_k \mathbf{y} \leq b_k, \forall k \in \{1, \dots, m\} \quad (19b)$$

$$\mathbf{x} \in \mathbb{Z}^n, \mathbf{y} \in \mathbb{R}^p, \quad (19c)$$

which will be used to represent the optimization problem of interest to this paper.

To make a ReLU network compatible with problem (19), we first consider that a neural network with $K + 1$ layers, with 0 being the input layer, and K the output layer. Each layer $k \in \{1, \dots, K\}$ has its output vector x^k calculated as:

$$x^k = \begin{cases} \sigma(W^k x^{k-1} + b^k), & \text{if } k \neq K \\ W^k x^{k-1} + b^k, & \text{otherwise} \end{cases}, \quad (20)$$

in which $\sigma(\cdot)$ is the ReLU activation function, given by:

$$\sigma(y) = \max\{0, y\}, \quad (21)$$

$W^k \in \mathbb{R}^{n_k \times n_{k-1}}$ is the matrix containing the weights of the neural network for each layer, and $b^k \in \mathbb{R}^{n_k}$ are the biases. Thus, we define $x^k \in \mathbb{R}^{n_k}$ as the output of layer k .

By following the methodology presented in [76], we can rewrite the ReLU operator as a MILP function [77], with the aid of big-M constraints:

$$W^k x^{k-1} + b^k = x^k - s^k \quad (22)$$

$$L^k \leq W^k x^{k-1} + b^k = x^k - s^k \leq U^k \quad (23)$$

Input: Parameters Θ , initial bounds B^-

$B \leftarrow B^-$

$k \leftarrow 0$

for $k \leq K$ **do**

$j \leftarrow 1$

for $j \leq n_k$ **do**

 Build set C_j^k based on Θ and B

 Solve for upper bound $u_j^k = \max(x_j^k - s_j^k)$ s.t. C_j^k

 Solve for lower bound $l_j^k = \min(x_j^k - s_j^k)$ s.t. C_j^k

 Update the bounds $B : U_j^k \leftarrow u_j^k$ and $L_j^k \leftarrow l_j^k$

$j \leftarrow j + 1$

end for

$k \leftarrow k + 1$

end for

return Updated bounds B

FIGURE 3 Bound tightening algorithm

$$x^k \leq U^k z^k \quad (24)$$

$$s^k \leq -L^k (1 - z^k) \quad (25)$$

$$z^k \in \{0, 1\}^{n_k}. \quad (26)$$

Notice that by means of (22), the ReLU is decoupled into a positive part ($x \geq 0$) and a negative part ($s \geq 0$). To obtain this behavior, at least one of the two terms is zero. This can be achieved by means of big-M constraints [78], assuming finite values of L and U as previously presented, with the aid of a binary variable z .

Thus, from an offline training of the neural network, its weight vector can be used as a constant input in a MILP optimization problem and solved in optimality [79]. In this paper, we represent the FEM output data as a MILP network to be inclusive in the optimization problem of interest.

Notice that the bounds defined by U and L can be tightened by an iterative process, as suggested by [76] and presented in Figure 3. The algorithm is an iterative procedure that updates the bounds of each neuron, layer by layer. It relies on solving subproblems in which the objective is to find the maximum (U) or minimum (L) value that a neuron can reach.

The summary of the procedure performed in this paper to optimize the spacer dimensions is presented in Figure 4. Initially, the component design was performed with a variation of distance parameters in the *SolidWorks* software, after the design, the files compatible with the *COMSOL Multiphysics* software were exported.

In the finite element software, the material, electrical potential application location, electrical potential value, and node mesh for simulation were defined. From the definitions of parameters for all the designs used, the simulation was carried out using FEM. The resulting FEM values were used as input to the optimization model, and thus, the optimized dimensions of the spacer were found. In this context, the optimal solution is

found when there is a convergence in the optimization model and the application of the defined dimensions results in a lower electric potential compared to the possible design variations.

4 | RESULTS AND DISCUSSION

Based on the finite element method, the visual results of applying the potential on conductors are presented. In the initial simulation, the distribution of electrical potential over the spacer surface is evaluated. As can be seen in Figure 5A, the color variation is related to the intensity of the applied electrical voltage along the surface.

The maximum value of this variation is 7.97 kV (RMS), which corresponds to the potential applied to each phase conductor with respect to ground. This electrical potential represents a phase-to-ground measurement in a 13.8 kV (phase-to-phase) three-phase delta system. Therefore, the value of 7.97 kV (RMS) is obtained by the ratio of $\sqrt{3}$ of in the 13.8 kV (RMS). With a greater electrical potential applied in a specific location, there is a greater chance of fault development since a greater potential per area results in a greater electrical field. With a greater electric

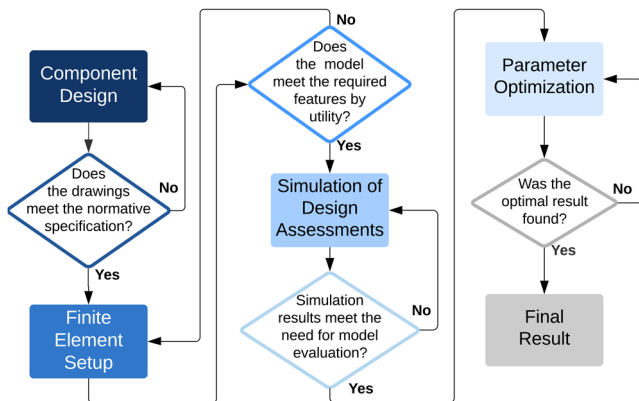


FIGURE 4 Flowchart of the proposed method

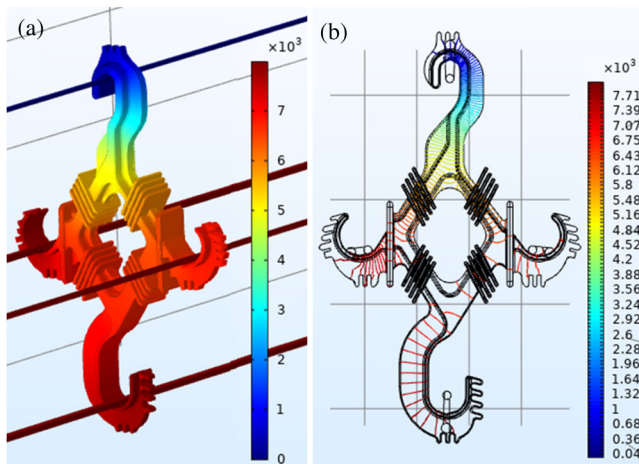


FIGURE 5 Electric potential: A) surface distribution; B) contour lines

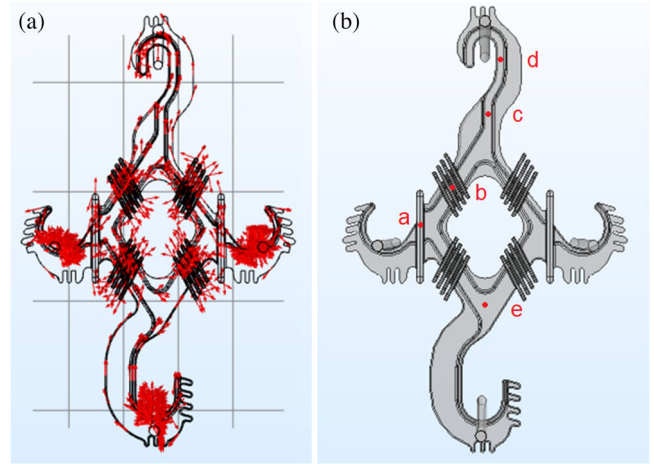


FIGURE 6 A) Electric field lines in the spacer; B) considered sites for the optimization

TABLE 2 Evaluation of the spacer height variation (vertical size)

| Vertical var. (mm) | Electrical potential (V) | | | | |
|--------------------|--------------------------|------|------|------|------|
| | a | b | c | d | e |
| 400 | 6856 | 6012 | 4139 | 1942 | 7114 |
| 402 | 6857 | 6013 | 4150 | 1961 | 7116 |
| 404 | 6865 | 6027 | 4182 | 2010 | 7122 |
| 406 | 6872 | 6037 | 4202 | 2037 | 7131 |
| 408 | 6858 | 6020 | 4192 | 2034 | 7112 |
| 410 | 6868 | 6036 | 4222 | 2075 | 7126 |
| 412 | 6863 | 6032 | 4236 | 2104 | 7116 |
| 414 | 6878 | 6054 | 4273 | 2151 | 7134 |
| 416 | 6892 | 6072 | 4299 | 2185 | 7143 |
| 418 | 6904 | 6082 | 4322 | 2219 | 7152 |

field, more partial discharges occur, consequently occur disruptive discharges.

The potential variation becomes clearer when the distribution of electric field by contour lines is analyzed, as shown in Figure 5B. The greater concentration of contour lines indicates more variations in potential levels, that is, more variation in applied electrical voltage.

The electrical potential is concentrated at equivalent levels in the regions close to the cables. The great difference in power distribution occurs in the region close to the messenger cable, which has a potential reference equal to zero. Figure 6A shows the comparison in relation to electric field lines. The field lines are presented in logarithmic scale, so it is possible to visualize the places where the differences are more expressive.

The critical locations where there is greater potential are around the conductors, these will be evaluated to perform an optimization of the model. Figure 6B shows the sites where this evaluation will be performed. The values of the electrical potential found from the variations in width and height are presented in Table 2.

TABLE 3 Evaluation of the spacer width variation (horizontal size)

| Horizontal var. (mm) | Electrical potential (V) | | | | |
|----------------------|--------------------------|------|------|------|------|
| | a | b | c | d | e |
| 255 | 6849 | 6003 | 4131 | 1939 | 7105 |
| 259 | 6841 | 5990 | 4127 | 1945 | 7096 |
| 263 | 6832 | 5977 | 4124 | 1950 | 7088 |
| 267 | 6799 | 5944 | 4112 | 1956 | 7064 |
| 271 | 6767 | 5912 | 4101 | 1960 | 7040 |
| 275 | 6763 | 5897 | 4087 | 1947 | 7031 |
| 279 | 6742 | 5877 | 4090 | 1971 | 7013 |
| 283 | 6693 | 5847 | 4074 | 1968 | 6995 |
| 293 | 6643 | 5816 | 4059 | 1965 | 6977 |
| 303 | 6644 | 5813 | 4086 | 2017 | 6979 |

The parameters of size variation were a 2 mm step increase for the vertical distance, from the smallest acceptable component height value (400 mm), and 4 mm variation for the first 8 values, and 10 mm for the last two. The 10 mm values were used in the last variations since the 4 mm variation did not generate representative variation results regarding the variation of the electric potential.

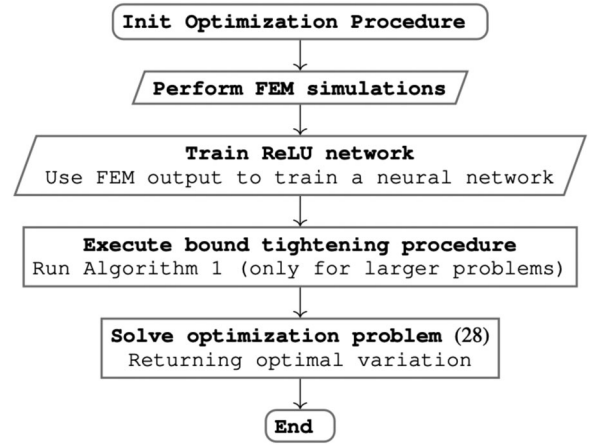
These initial analysis parameters were used according to the definitions of the spacer used by the local electricity utility. For the horizontal and vertical variations, 10 pieces were used as can be seen in Table 3, and when variations were made in one of the coordinates, the other was fixed at the minimum value determined by the local electricity utility.

4.1 | Parameter optimization

Following the methodology previously presented, we write the problem of interest as an MILP, where the data from FEM simulations are used to train neural networks with ReLU activation function. The experiments were implemented in Python 3.6. The training of networks consisted of a dataset of 10,000 points, considering a split of 70/30 for the training/validation of the networks. Notice that, typically, MILP problems can be solved to optimality or near optimality (within a dual gap) by exact algorithms such as branch-and-bound [80] or approximated using heuristics. In this this paper, the solver Gurobi v9.0 [81] was used to solve the MILP problems to optimality. They experiments were run in a Ubuntu environment, and the computer had two Intel Core Xeon E5-2630 v4 Processors (2.20 GHz), adding up to 20 cores of 2 threads and 64 GB of RAM.

The problem of interest consists in finding the variation which minimizes the sum of the electrical potential in all the evaluated spots:

$$\min \sum_{i=a}^e V_i \quad (27a)$$

**FIGURE 7** Optimization procedure

$$\text{s.t. } V^{i,\min} \leq V^i \leq V^{i,\max}, i \in \{a, \dots, e\}, \quad \forall k = 0 \quad (27b)$$

$$W^k x^{k-1} + b^k = x^k - s^k, \quad \forall k = 1, \dots, K-1 \quad (27c)$$

$$x^k \leq U^k \tilde{x}^k, \quad \forall k = 1, \dots, K-1 \quad (27d)$$

$$s^k \leq -L^k(1 - \tilde{x}^k), \quad \forall k = 1, \dots, K-1 \quad (27e)$$

$$\tilde{x}^k \in \{0, 1\}^{n^k}, \quad \forall k = 1, \dots, K-1 \quad (27f)$$

$$L^k \geq x^k - s^k, \quad \forall k = 1, \dots, K-1 \quad (27g)$$

$$x^k - s^k \leq U^k, \quad \forall k = 1, \dots, K-1 \quad (27h)$$

$$W^K x^{K-1} + b^K = \text{var}, \quad \forall k = K \quad (27i)$$

$$\text{var}^{\min} \leq \text{var} \leq \text{var}^{\max}, \quad \forall k = K. \quad (27j)$$

Notice that the neural network is trained by considering the electrical potentials as inputs (V) and the vertical/horizontal variations as outputs (var) since the optimization problem is able to handle the maximization/minimization of the inputs. Also, Equation (27) can be easily adapted to consider additional constraints or bounds in the project dimensions. Overall, the optimization procedure used in this paper can be summarized as presented in Figure 7 [82].

4.1.1 | Vertical size

First, we consider the problem of the spacer height variation (vertical size). For that, we considered a structural test presented in Figure 8 (varying the number of layers and neurons). From

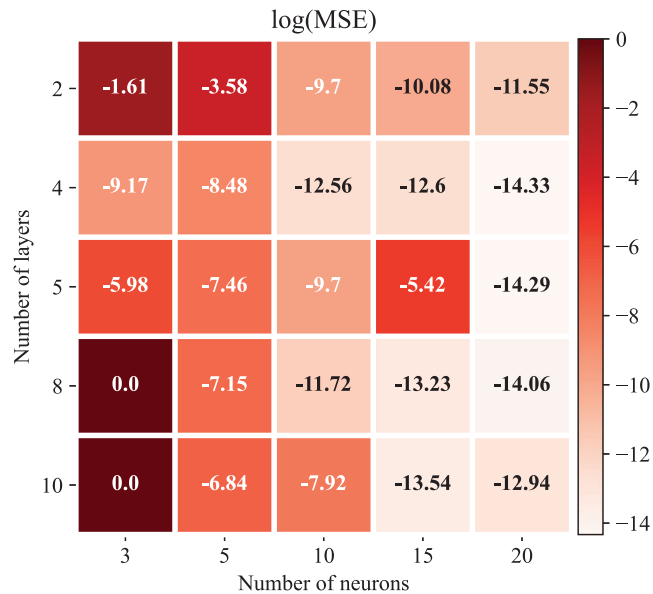


FIGURE 8 Structural test for the ReLU network with data from vertical variation

the structural test, the network containing 5 layers with 20 neurons each was selected in order to be considered for the optimization model, which after solving (27) suggests the vertical variation of 400 mm. The 400 mm vertical variation results in an electrical potential of $a = 6856\text{V}$, $b = 6012\text{V}$, $c = 4139\text{V}$, $d = 1942\text{V}$ and $e = 7114\text{V}$.

4.1.2 | Horizontal size

Second, we consider the problem regarding the spacer width variation (horizontal size). First, we performed a structural test varying the number of layers and neurons, as shown in Figure 9. After solving (27) for the best found neural network (considering 4 layers with 10 neurons each), the suggested horizontal variation is defined as 290.55 mm. The suggested horizontal variation results in an electrical potential of $a = 6643\text{V}$, $b = 5813\text{V}$, $c = 4059\text{V}$, $d = 1939\text{V}$ and $e = 6977\text{V}$.

5 | CONCLUSION

As the compact grid is new and is being developed, more definitions of the constructive characteristics are necessary. Based on this need to improve the design of components used in this type of network, developing prototypes, and submitting them to computational analysis through FEM is promising. From this analysis, it is possible to design components that are more reliable and robust, while using a minimal amount of material.

The FEM proved to be able to highlight important variations for the development of prototypes and studies of distribution network components. From the FEM, the design is optimized considering a ReLU neural network as a substitution model. The versatility of the method allows working with high

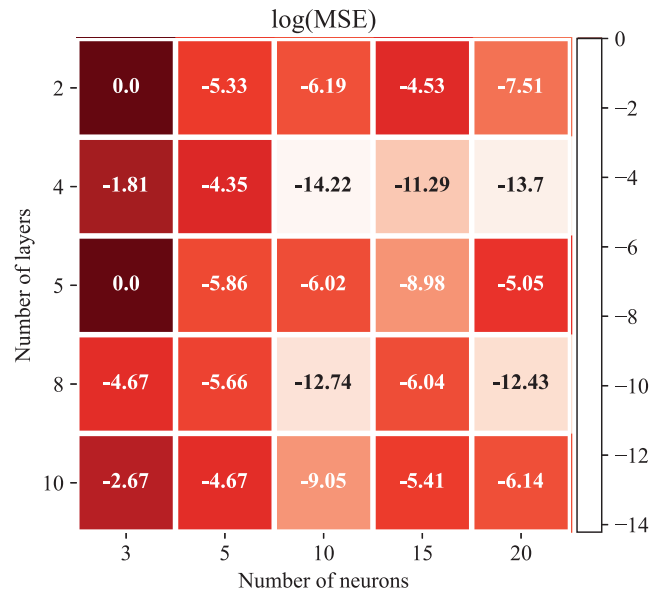


FIGURE 9 Structural test for the ReLU network with data from horizontal variation

dimensionality of input and output parameters, making the optimization problem grow only in binary proportional to the number of neurons, unlike traditional techniques such as piecewise-linearization. Furthermore, rewriting the problem as an MILP allows the operator to easily add and manipulate new constraints and limits.

The results highlighted that design variation should be evaluated to improve potential distribution in distribution spacers. This statement is supported mainly in relation to the result of variation “d”, which had a difference of 14.26% higher potential at this site. This position is close to the conductor and for this reason, it presented more variation and requires more attention in the design project. Using the proper neural network parameter configuration, the model converges resulting in optimization with close to zero error in both the vertical and horizontal variation of the spacer profile.

In future analysis, temperature and humidity variations can be explored using FEM, these factors can influence the electrical potential isolation capacity of components of the power distribution network. In addition, it is possible to analyze the influence of contaminations, considering that their accumulation on the surface of the components can make it more conductive, resulting in a greater vulnerability to the spacer, since there will be more leakage current on the contaminated surface, resulting in dielectric rupture.

ACKNOWLEDGEMENTS

This work was supported by national funds through the Fundação para a Ciência e a Tecnologia, I.P. (Portuguese Foundation for Science and Technology) by the project UIDB/05064/2020 (VALORIZA—Research Centre for Endogenous Resource Valorization), and Project UIDB/04111/2020, ILIND—Instituto Lusófono de Investigação e Desenvolvimento, under project

COFAC/ILIND/ COPELABS/3/2020. Fundación M. D. Samuel Solórzano Barruso, Proyecto Solórzano FS/27-2020.

CONFLICT OF INTEREST

We have no conflict of interest.


PERMISSION TO REPRODUCE MATERIALS FROM OTHER SOURCES

None.

DATA AVAILABILITY STATEMENT

The data is available through the request to the first author.

ORCID

Stéfano Frizzo Stefenon  <https://orcid.org/0000-0002-3723-616X>

Laio Oriel Seman  <https://orcid.org/0000-0002-6806-9122>

Bruno Antonio Pavan  <https://orcid.org/0000-0002-9161-0319>

Raúl García Ovejero  <https://orcid.org/0000-0002-2862-3053>

Valderi Reis Quietinbo Leithardt  <https://orcid.org/0000-0003-0446-9271>

REFERENCES

- Al Nory, M.T.: Optimal decision guidance for the electricity supply chain integration with renewable energy: Aligning smart cities research with sustainable development goals. *IEEE Access* 7, 74996–75006 (2019)
- Shan, S., Cao, B., Wu, Z.: Forecasting the short-term electricity consumption of building using a novel ensemble model. *IEEE Access* 7, 88093–88106 (2019)
- Santos, S., Richart, F., da Silva, G., Kowalski, E., Ribeiro, S., Dadam, A., et al.: Spacer design for 15 kv compact overhead distribution networks for regions with high environmental aggressiveness. *IEEE Lat. Am. Trans.* 16(10), 2634–2641 (2018)
- Stefenon, S.F., Ribeiro, M.H.D.M., Nied, A., Mariani, V.C., Coelho, L.S., Leithardt, V.R.Q., et al.: Hybrid wavelet stacking ensemble model for insulators contamination forecasting. *IEEE Access* 9, 66387–66397 (2021)
- Zhu, W., Dong, G., Yang, Y.: Thermal-aware modeling and analysis for a power distribution network including through-silicon-vias in 3-d ics. *IEEE Trans. Comp.-Aided Design Integrated Circuits Syst.* 38(7), 1278–1290 (2019)
- Aouabed, F., Bayadi, A., Rahmani, A.E., Boudissa, R.: Finite element modelling of electric field and voltage distribution on a silicone insulating surface covered with water droplets. *IEEE Trans. Dielectr. Electr. Insul.* 25(2), 413–420 (2018)
- Sun, Y., Su, B., Sun, X.: Optimal design and performance analysis for interior composite-rotor bearingless permanent magnet synchronous motors. *IEEE Access* 7, 7456–7465 (2019)
- Orosz, T., Rassölkin, A., Kallaste, A., Arsénio, P., Pánek, D., Kaska, J., et al.: Robust design optimization and emerging technologies for electrical machines: Challenges and open problems. *Appl. Sci.* 10(19), 6653 (2020)
- Lee, J.H., Kim, J.W., Song, J.Y., Kim, D.W., Kim, Y.J., Jung, S.Y.: Distance-based intelligent particle swarm optimization for optimal design of permanent magnet synchronous machine. *IEEE Trans. Magn.* 53(6), 1–4 (2017)
- Lee, K.I., Oh, H.S., Jung, S.H., Chung, Y.S.: Moving least square-based hybrid genetic algorithm for optimal design of W -band dual-reflector antenna. *IEEE Trans. Magn.* 55(6), 1–4 (2019)
- Wang, X., Xia, Z., Zhou, X., Guo, Y., Gu, X., Yan, H.: Multiobjective path optimization for arc welding robot based on dmoea/d-et algorithm and proxy model. *IEEE Trans. Instrum. Meas.* 70, 1–13 (2021)
- Kumar, A., Das, S., Mallipeddi, R.: A reference vector-based simplified covariance matrix adaptation evolution strategy for constrained global optimization. *IEEE Trans. Cybern.* 1–14 (2020)
- Bajaj, M., Sharma, N.K., Pushkarna, M., Malik, H., Alotaibi, M.A., Almutairi, A.: Optimal design of passive power filter using multi-objective pareto-based firefly algorithm and analysis under background and load-side's nonlinearity. *IEEE Access* 9, 22724–22744 (2021)
- Chitara, D., Niazi, K.R., Swarnkar, A., Gupta, N.: Cuckoo search optimization algorithm for designing of a multimachine power system stabilizer. *IEEE Trans. Ind. Appl.* 54(4), 3056–3065 (2018)
- Feng, T., He, W., Wang, J.G.: Fem simulation of charge accumulation behaviours on polyimide surface in 10 kv negative high-voltage corona polarization process. *IEEE Access* 8, 113151–113162 (2020)
- Yin, F., Dang, K., Yang, W., Ding, Y., Xie, P.: Feature-integrated structural optimization design method and performance evaluation for hollow slab structures. *IEEE Access* 8, 220450–220460 (2020)
- Stefenon, S.F., Seman, L.O., Sopelsa Neto, N.F., Meyer, L.H., Nied, A., Yow, K.C.: Echo state network applied for classification of medium voltage insulators. *Int. J. Electr. Power Energy Syst.* 134, 107336 (2022)
- Sopelsa Neto, N.F., Stefenon, S.F., Meyer, L.H., Bruns, R., Nied, A., Seman, L.O., et al.: A study of multilayer perceptron networks applied to classification of ceramic insulators using ultrasound. *Appl. Sci.* 11(4), 1592 (2021)
- Dong, M., Wang, B., Ren, M., Zhang, C., Zhao, W., Albarracín, R.: Joint visualization diagnosis of outdoor insulation status with optical and acoustical detections. *IEEE Trans. Power Delivery* 34(4), 1221–1229 (2019)
- Diamantis, A., Kladas, A.G.: Mixed numerical methodology for evaluation of low-frequency electric and magnetic fields near power facilities. *IEEE Trans. Magn.* 55(6), 1–4 (2019)
- Li, N., Mao, J., Zhao, W.S., Tang, M., Yin, W.Y.: High-frequency electrothermal characterization of tsv-based power delivery network. *IEEE Trans. Compon. Packag. Manuf. Technol.* 8(12), 2171–2179 (2018)
- Yang, W., Peng, F., Dinavahi, V., Zhai, G.: A generalized parallel transmission line iteration for finite element analysis of permanent magnet axisymmetrical actuator. *IEEE Trans. Magn.* 55(3), 1–10 (2019)
- Li, J., Liu, P., Dinavahi, V.: Massively parallel computation for 3-d nonlinear finite edge element problem with transmission line decoupling technique. *IEEE Trans. Magn.* 55(10), 1–8 (2019)
- Stefenon, S.F., Freire, R.Z., Meyer, L.H., Corso, M.P., Sartori, A., Nied, A., et al.: Fault detection in insulators based on ultrasonic signal processing using a hybrid deep learning technique. *IET Sci. Meas. Technol.* 14(10), 953–961 (2020)
- Zhang, Z., Qiao, X., Xiang, Y., Jiang, X.: Comparison of surface pollution flashover characteristics of rtv (room temperature vulcanizing) coated insulators under different coating damage modes. *IEEE Access* 7, 40904–40912 (2019)
- Guo, Z., Wu, Z., Wang, H., Tian, H., Liu, L., Peng, Z., et al.: Experimental and numerical study on formation of interface separation and interfacial dielectric strength of gil insulator. *IEEE Trans. Dielectr. Electr. Insul.* 26(6), 1738–1746 (2019)
- Deb, S., Ray Choudhury, N., Ghosh, R., Chatterjee, B., Dalai, S.: Short time modified hilbert transform-aided sparse representation for sensing of overhead line insulator contamination. *IEEE Sens. J.* 18(19), 8125–8132 (2018)
- Qiao, X., Zhang, Z., Jiang, X., He, Y., Li, X.: Application of grey theory in pollution prediction on insulator surface in power systems. *Eng. Fail. Anal.* 106, 104153 (2019)
- Zhang, D., Chen, S.: Intelligent recognition of insulator contamination grade based on the deep learning of ultraviolet discharge image information. *Energies* 13(19), 5221 (2020)
- Salem, A.A., Abd Rahman, R., Al Gailani, S.A., Kamarudin, M.S., Ahmad, H., Salam, Z.: The leakage current components as a diagnostic tool to estimate contamination level on high voltage insulators. *IEEE Access* 8, 92514–92528 (2020)
- Kim, S., Kim, Y., Cho, K., Song, J., Kim, J.: Design and measurement of a novel on-interposer active power distribution network for efficient simultaneous switching noise suppression in 2.5-d/3-d ic. *IEEE Trans. Compon. Packag. Manuf. Technol.* 9(2), 317–328 (2019)
- Ghiasi, Z., Faghihi, F., Shayegani Akmal, A.A., CheshmehBeigi, H.M., Rouzbehi, K.: Fem analysis of electric field distribution for polymeric

- insulator under different configuration of non-uniform pollution. *Electr. Eng.* 103, 2799–2808 (2021)
33. Salem, A.A., Abd Rahman, R., Rahiman, W., Al Gailani, S.A., Al Ameri, S.M., Ishak, M.T., et al.: Pollution flashover under different contamination profiles on high voltage insulator: Numerical and experiment investigation. *IEEE Access* 9, 37800–37812 (2021)
 34. Orosz, T., Pánek, D., Karban, P.: Fem based preliminary design optimization in case of large power transformers. *Appl. Sci.* 10(4), 1361 (2020)
 35. Zhang, Y., Lu, T.: Unsteady-state thermal stress and thermal deformation analysis for a pressurizer surge line subjected to thermal stratification based on a coupled cfd-fem method. *Ann. Nuclear Energy* 108, 253–267 (2017)
 36. Mou, Z., Yan, B., Lin, X., Huang, G., Lv, X.: Prediction method for galloping features of transmission lines based on fem and machine learning. *Cold Reg. Sci. Technol.* 173, 103031 (2020)
 37. Farah, A.A.M., Afonso, M.M., Vasconcelos, J.A., Schroeder, M.A.O.: A finite-element approach for electric field computation at the surface of overhead transmission line conductors. *IEEE Trans. Magn.* 54(3), 1–4 (2018)
 38. Paul, S., Chang, J.: Design of novel electromagnetic energy harvester to power a deicing robot and monitoring sensors for transmission lines. *Energy Convers. Manage.* 197, 111868 (2019)
 39. Ayodele, T.R., Ogunjuyigbe, A.S.O., Oyewole, O.E.: Comparative assessment of the effect of earthing grid configurations on the earthing system using ieee and finite element methods. *Eng. Sci. Technol.* 21(5), 970–983 (2018)
 40. Qi, L., Cui, X., Zhao, Z., Li, H.: Grounding performance analysis of the substation grounding grids by finite element method in frequency domain. *IEEE Trans. Magn.* 43(4), 1181–1184 (2007)
 41. Rawashdeh, M.R., Rosell, A., Udpa, L., Hoole, S.R.H., Deng, Y.: Optimized solutions for defect characterization in 2-d inverse eddy current testing problems using subregion finite element method. *IEEE Trans. Magn.* 54(8), 1–15 (2018)
 42. Jeong, C.L., Kim, Y.K., Hur, J.: Optimized design of pmsm with hybrid-type permanent magnet for improving performance and reliability. *IEEE Trans. Ind. Appl.* 55(5), 4692–4701 (2019)
 43. Aiello, G., Gagliardi, M., Meier, A., Saibene, G., Scherer, T.A., Schreck, S., et al.: Iter torus diamond window unit: Fem analyses and impact on the design. *IEEE Trans. Plasma Sci.* 47(7), 3289–3297 (2019)
 44. Zaccaria, C., Mancinelli, M., Pavesi, L.: A fem enhanced transfer matrix method for optical grating design. *J. Lightwave Technol.* 39(11), 3521–3530 (2021)
 45. Mohammed, M.S., Vural, R.A.: Nsga-ii+fem based loss optimization of three-phase transformer. *IEEE Trans. Ind. Electron.* 66(9), 7417–7425 (2019)
 46. Qiao, J., Zou, J., Yuan, J., Lee, J., Ju, M.n.: Method of local characteristics for calculating electric field and ion current of hvdc transmission lines with transverse wind. *IET Gener. Transm. Distrib.* 11(4), 1055–1062 (2017)
 47. Tian, H., Liu, P., Zhou, S., Wang, Q., Wu, Z., Zhang, J., et al.: Research on the deterioration process of electrical contact structure inside the ± 500 kv converter transformer rip bushings and its prediction strategy. *IET Gener. Transm. Distrib.* 13(12), 2391–2400 (2019)
 48. Ramirez Vazquez, I., Espino Cortes, F.P.: Electric-field analysis of spacer cable systems for compact overhead distribution lines. *IEEE Trans. Power Delivery* 27(4), 2312–2317 (2012)
 49. Espino Cortes, F.P., Ramirez Vazquez, I., Gomez, P., Heredia, V.: Performance of a spacer cable system under polluted conditions. *IEEE Electr. Insul. Mag.* 30(6), 13–19 (2014)
 50. El Shaarawy, Z., Talaat, M., El Zein, A.: Field reduction simulation based on covered conductors design in medium voltage lines. *Results Eng.* 10, 100217 (2021)
 51. Coster, E.J., Myrzik, J.M.A., Kruimer, B., Kling, W.L.: Integration issues of distributed generation in distribution grids. *Proc. IEEE* 99(1), 28–39 (2011)
 52. Arantes Monteiro, R.V., Caixeta Guimaraes, G., Manoel Batista da Silva, A., Tamashiro, M.A., Bento Silva, F.: Three - phase analysis of active losses on conventional and compact distribution networks. *IEEE Lat. Am. Trans.* 15(4), 682–689 (2017)
 53. Thomas, A.J., C, I., Reddy, C.C.: A method for surface voltage measurement of an overhead insulated conductor. *IEEE Trans. Instrum. Meas.* 70, 1–8 (2021)
 54. Huangfu, Y., Wang, S., Wang, G., Xu, W., Zhang, H.: Modeling and insulation performance analysis of composite transmission line tower under lightning overvoltage. *IEEE Trans. Magn.* 51(3), 1–4 (2015)
 55. 313..0045, E.: Distribution systems development system subsystem standards and studies of distribution materials and equipment: Product approval certification. *Special Manual (Celesc)* 1, 1–44 (2020)
 56. Edwards, T.C., Steer, M.B.: Foundations for microstrip circuit design. In: Appendix B: Material Properties, pp. 635–642. John Wiley & Sons, Hoboken (2016). <https://onlinelibrary.wiley.com/doi/abs/10.1002/9781118936160.app2>
 57. Lin, S., Chen, L., Zhang, H., Zhou, Q.: Fem with curved hexahedron element and application on tunnel integrated grounding system in high-speed railway. *IEEE Trans. Veh. Technol.* 68(7), 6441–6452 (2019)
 58. De La Hoz, M., Etxegarai, A., Larrea, A.M., Mazon, A.J., Zorrozuza, M.A.: Impact assessment of clearance in corona testing for a high-voltage substation connector set using fem. *IET Gener. Transm. Distrib.* 14(18), 3710–3718 (2020)
 59. Yadollahi, M., Lesani, H.: Power transformer optimal design using an innovative heuristic algorithm combined with mixed-integer non-linear programming and fem technique. *IET Gener. Transm. Distrib.* 11(13), 3359–3370 (2017)
 60. Talaat, M., Tayseer, M., El Zein, A.: Digital image processing for physical basis analysis of electrical failure forecasting in xlpe power cables based on field simulation using finite-element method. *IET Gener. Transm. Distrib.* 14(26), 6703–6714 (2020)
 61. Yang, Z., Ruan, J., Huang, D., Du, Z., Tang, L., Zhou, T.: Calculation of hot spot temperature of transformer bushing considering current fluctuation. *IEEE Access* 7, 120441–120448 (2019)
 62. Stefenon, S.F., Seman, L.O., Furtado Neto, C.S., Nied, A., Seganfredo, D.M., Luz, F.G., et al.: Electric field evaluation using the finite element method and proxy models for the design of stator slots in a permanent magnet synchronous motor. *Electronics* 9(11), 1975 (2020)
 63. Feng, T., He, W., Wang, J.G.: Fem simulation of charge accumulation behavior on polyimide surface in 10 kv negative high-voltage corona polarization process. *IEEE Access* 8, 113151–113162 (2020)
 64. Farah, A.A.M., Afonso, M.M., Vasconcelos, J.A., Schroeder, M.A.O.: A finite-element approach for electric field computation at the surface of overhead transmission line conductors. *IEEE Trans. Magn.* 54(3), 7400904 (2018)
 65. Stefenon, S., Nied, A.: Fem applied to evaluation of the influence of electric field on design of the stator slots in pmsm. *IEEE Lat. Am. Trans.* 17(04), 590–596 (2019)
 66. Hu, X., Wang, Z., Tian, R.: Calculation of the dynamic wind-induced deflection response of overhead lines: Establishment and analysis of the multi-rigid-body model. *IEEE Access* 8, 180883–180895 (2020)
 67. Stefenon, S.F., Neto, C.S.F., Coelho, T.S., Nied, A., Yamaguchi, C.K., Yow, K.C.: Particle swarm optimization for design of insulators of distribution power system based on finite element method. *Electr. Eng.*, 2021, pp. 1–8
 68. Salem, A.A., Abd Rahman, R., Rahiman, W., Al Gailani, S.A., Al Ameri, S.M., Ishak, M.T., et al.: Pollution flashover under different contamination profiles on high voltage insulator: Numerical and experiment investigation. *IEEE Access* 9, 37800–37812 (2021)
 69. Anbarasan, R., Usa, S.: Electrical field computation of polymeric insulator using reduced dimension modeling. *IEEE Trans. Dielectr. Electr. Insul.* 22(2), 739–746 (2015)
 70. Vajdi, M., Moghanlou, F.S., Sharifianjazi, F., Asl, M.S., Shokouhimehr, M.: A review on the comsol multiphysics studies of heat transfer in advanced ceramics. *J. Compos. Comp.* 2(2), 35–43 (2020)
 71. Rai, A.: Explainable ai: From black box to glass box. *J. Acad. Marketing Sci.* 48(1), 137–141 (2020)
 72. Zhao, W., Gupta, A., Regan, C.D., Miglani, J., Kapania, R.K., Seiler, P.J.: Component data assisted finite element model updating of composite

- flying-wing aircraft using multi-level optimization. *Aerosp. Sci. Technol.* 95, 105486 (2019)
73. Wang, S., Hua, L., Yang, C., Han, X., Su, Z.: Applications of incremental harmonic balance method combined with equivalent piecewise linearization on vibrations of nonlinear stiffness systems. *J. Sound Vib.* 441, 111–125 (2019)
74. Camponogara, E., Nazari, L.F.: Models and algorithms for optimal piecewise-linear function approximation. *Math. Prob. Eng.* 2015(876862), 1–9 (2015)
75. Yang, Q., Sadeghi, A., Wang, G., Sun, J.: Learning two-layer relu networks is nearly as easy as learning linear classifiers on separable data. *IEEE Trans. Signal Process.* 69, 4416–4427 (2021)
76. Grimstad, B., Andersson, H.: Relu networks as surrogate models in mixed-integer linear programs. *Comput. Chem. Eng.* 131, 106580 (2019)
77. Wang, X., Brandt Pearce, M., Subramaniam, S.: Impact of wavelength and modulation conversion on translucent elastic optical networks using milp. *J. Opt. Commun. Networking* 7(7), 644–655 (2015)
78. Liu, J., Liu, S.: Optimal distributed generation allocation in distribution network based on second order conic relaxation and big-m method. *Power Syst. Technol.* 42(8), 2604–2611 (2018)
79. Zatti, M., Gabba, M., Freschini, M., Rossi, M., Gambarotta, A., Morini, M., et al.: k-milp: A novel clustering approach to select typical and extreme days for multi-energy systems design optimization. *Energy* 181, 1051–1063 (2019)
80. Vanderbei, R.J.: Linear programming. In: *International Series in Operations Research & Management Science*, vol. 37. Springer, Boston (2001)
81. Gurobi Optimization, LLC: Gurobi optimizer reference manual. <http://www.gurobi.com>. Accessed 4 February 2022
82. Abadi, M., Barham, P., Chen, J., Chen, Z., Davis, A., Dean, J., et al.: TensorFlow: A system for large-scale machine learning. In: *Proceedings of the 12th USENIX Conference on Operating Systems Design and Implementation*, pp. 265–283. USENIX Association, Berkeley (2016). <https://www.tensorflow.org/>

How to cite this article: Stefenon, S.F., Seman, L.O., Pavan, B.A., Ovejero, R.G., Leithardt, V.Q.: Optimal design of electrical power distribution grid spacers using finite element method. *IET Gener. Transm. Distrib.* 1–12 (2022). <https://doi.org/10.1049/gtd2.12425>